EARTHQUAKE ENGINEERING AND STRUCTURAL DYNAMICS
Earthquake Engng. Struct. Dyn. **28**, 1383–1403 (1999)

DYNAMIC SOIL–STRUCTURE INTERACTION EFFECTS ON THE SEISMIC RESPONSE OF SUSPENSION BRIDGES

MANISH SHRIKHANDE[1†] AND VINAY K. GUPTA[2*‡]

[1] *Department of Earthquake Engineering, University of Roorkee, Roorkee-247667, India*
[2] *Department of Civil Engineering, Indian Institute of Technology, Kanpur-208016, India*

SUMMARY

A stochastic approach has been formulated for the linear analysis of suspension bridges subjected to earthquake excitations. The transfer functions of various responses have been formulated while including the effects of dynamic Soil–Structure Interaction (SSI) via the use of the fixed-base modes of the structure. The excitation has been characterized by the 'equivalent stationary' processes corresponding to the free-field motions at each support and by an assumed coherency function between these motions. The proposed formulation considers the non-stationarity in the structural response due to sudden application of excitation by considering (i) the time-dependent frequency response functions, and (ii) the order statistics formulation for the peak factors in evolutionary response processes. The formulation has been illustrated by analysing the seismic response of the Golden Gate bridge at San Francisco for two example excitations conforming to USNRC-specified design spectra. The significance of various governing parameters on the dynamic soil–structure interaction effects on the seismic response of suspension bridges has also been studied. It has been found that the contribution of the vertical component of ground motion to the bridge response increases with increasing soil compliance. Also, the extent to which the spatial variation of ground motion affects the bridge response depends on how significant the SSI effects are. Copyright © 1999 John Wiley & Sons Ltd.

KEY WORDS: suspension bridges; equivalent stationary excitation; nonstationary seismic response; dynamic soil–structure interaction; fixed-base modes; coherency function

1. INTRODUCTION

Bridges are critical life-line facilities which should remain functional without damage after an earthquake to facilitate the rescue and relief operations. Among the various structural forms available for the bridges, suspension bridges have been the focus of several past studies on the seismic response of bridges. Abdel-Ghaffar and Rubin[1,2] studied the effects of asynchronous multi-support seismic excitations on the suspension bridge vibrations in the vertical plane by using a stationary random vibration analysis. They concluded that the uncorrelated ground

* Correspondence to: Vinay K. Gupta, Department of Civil Engineering, Indian Institute of Technology, Kanpur, 208016, India
† Lecturer
‡ Associate Professor

Received 24 August 1998
Revised 17 March 1999
Accepted 21 June 1999

CCC 0098–8847/99/111383–21$17·50
Copyright © 1999 John Wiley & Sons, Ltd.

motions overestimate the bridge response and that the assumption of uniform ground motion over the entire span does not represent the critical loading. Further, they observed that it was necessary to retain a large number of modes in the modal summation to capture the response features accurately. Abdel-Ghaffar and Stringfellow[3,4] studied the effect of wave propagation on the seismic response of suspension bridges and concluded that the apparent velocity of propagation can have a significant effect on the bridge response. Dumanoglu and Severn[5] compared the response of suspension bridges to synchronous seismic excitations as obtained from a stationary random vibration analysis with that from a time-history analysis and highlighted the possible errors in the stochastic response calculations due to the assumption of stationarity of response. Hyun *et al.*[6] proposed a method for the non-stationary random vibration analysis of suspension bridges subjected to the multi-support seismic excitations. They found that while the correlation effects significantly influence the response characteristics, the effect of longitudinal earthquake components on the response of suspension bridge in vertical plane is more significant than that of the vertical components. The inadequacy of the stationary random vibration analysis in the case of suspension bridges has also been pointed out in a recent study by Harichandran *et al.*[7] They compared the lateral response of a suspension bridge obtained by using a general spatially varying earthquake ground motion model with the response computed by using the identical and delayed excitations, and found that the use of delayed or uniform excitation underestimates the seismic response of a long-span suspension bridge. Betti *et al.*[8] showed that the seismic response of suspension bridges can be significantly altered by the effects of kinematic Soil–Structure Interaction (SSI).

All the above-mentioned studies have been based on the assumption that the effects of dynamic or inertial SSI on the bridge response are small. However, these effects on the response of tower can be significantly large as shown by Yamada *et al.*[9] in case of a soil–bridge pier sub-system. There has been no study which considers the seismic response of the bridge while including the effects of dynamic SSI. Hence, it becomes necessary to formulate such a response and to study the extent to which this may deviate from the fixed-base response.

A dynamic SSI analysis in time domain is usually carried out by idealizing the soil compliance through springs and dashpots whose properties are independent of the frequency of excitation. For the linear systems, however, it is possible to account for the frequency dependence of the soil springs and dashpots (as implied by the impedance functions of the foundation) by carrying out the analysis in frequency domain. In this, it is generally considered convenient to describe the structure response in terms of its (undamped) fixed-base mode shapes.[10–13] As shown by Gupta and Trifunac,[13] it may even be possible to account for the dynamic SSI effects by analysing the fixed-base structure for a modified foundation motion which represents the free-field ground motion modified to include the motion of foundation relative to the surrounding soil medium.

In this study, we propose a stochastic approach for the seismic response of suspension bridges while including the effects of dynamic SSI. For this, the modified excitation approach of Gupta and Trifunac[13] has been used, and the non-stationarity in the response process has been accounted for by a simple extension of a recent formulation of Shrikhande and Gupta.[14] For simplicity, only the suspension bridge vibrations in the vertical plane have been considered. The three-span, Golden Gate suspension bridge has been considered along with two example excitations to illustrate the proposed approach. Further, the effects of kinematic interaction have been ignored, and the impedance functions given by Pais and Kausel[15] and the ground motion spatial variability model proposed by Hindy and Novak[16] have been employed. The proposed approach is then used to study the significance of dynamic SSI effects on the seismic response of

Copyright © 1999 John Wiley & Sons, Ltd.

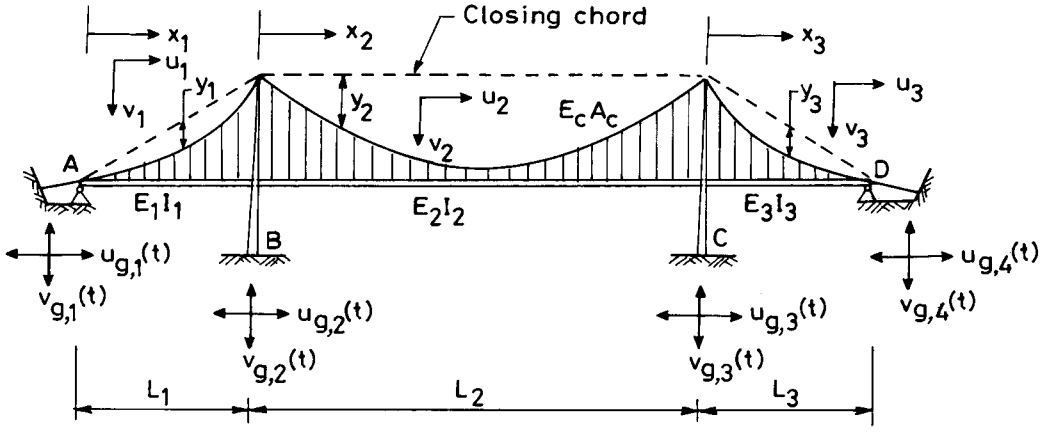

Figure 1. Schematic diagram of a three-span suspension bridge

suspension bridges. This has been done with focus on the modification of the free-field ground motions and the effects of the spatially varying ground motions on seismic response.

2. VERTICAL VIBRATION OF A SUSPENSION BRIDGE: A REVIEW

Let us consider a typical three-span suspension bridge as shown in Figure 1. The dead load and the flexural stiffness of the stiffening girder are assumed to be constant throughout each span and the suspenders are considered to be inextensible so that the vertical deflections of the cable and the stiffening girder can be assumed to be identical. Further, on assuming small amplitude vibrations and neglecting the change in the cable tension due to the inertia forces in comparison with the initial cable tension due to the dead loads, the equations of motion for the vibration of suspension bridge can be linearized. Moreover, the coupling of the vertical and torsional vibrations is eliminated due to the linearization of the equations of motion.[17] Thus, the equations of motion for the vibration of the ith span of the suspension bridge in the vertical plane may be written as,[1,2]

$$\frac{w_i}{g}\frac{\partial^2 v_i}{\partial t^2} + C_i\frac{\partial v_i}{\partial t} + E_i I_i\frac{\partial^4 v_i}{\partial x_i^4} - H_w\frac{\partial^2 v_i}{\partial x_i^2} + \frac{w_i}{H_w}H(t) = 0, \quad i = 1, 2, 3 \tag{1}$$

where w_i is the dead weight, including weight of deck and that of the cables, per unit length of the ith span, $v_i = v_i(x_i, t)$ represents the absolute vertical displacement of a point on the deck of the ith span of the bridge, C_i denotes the coefficient of the velocity-proportional dissipation force in the ith span, E_i and I_i denote the Young's modulus and the moment of inertia, respectively, for the ith stiffening girder, H_w is the horizontal component of the initial cable tension (due to the dead loads), $H(t)$ is the horizontal component of additional (vibrational) cable tension, given by

$$H(t) = \frac{E_c A_c}{L_e}\sum_{i=1}^{3}\left[u_c(x_i, t)\Big|_0^{L_i} + \frac{\mathrm{d}y_i}{\mathrm{d}x_i}v_i\Big|_0^{L_i} + \frac{w_i}{H_w}\int_0^{L_i} v_i(x_i, t)\,\mathrm{d}x_i\right] \tag{2}$$

Copyright © 1999 John Wiley & Sons, Ltd.

Here, E_c, A_c are the Young's modulus of elasticity and the cross-sectional area, respectively, of the cables, L_e represents the virtual length of the cables and is defined as the length of the equivalent truss element with the same strain energy, area of cross-section and the modulus of elasticity as that of the suspension cables subjected to a constant axial force equal to the horizontal component of the dynamic component of the cable tension, $H(t)$ (see Reference 18 for more details), $u_c(x_i, t)$ is the absolute longitudinal cable displacement, L_i denotes the length of the ith span, and $y_i = y_i(x_i)$ is the cable ordinate measured vertically from the closing chord of the ith span (see Figure 1), given by

$$y_i = \frac{w_i L_i^2}{2H_w}\left[\frac{x_i}{L_i} - \left(\frac{x_i}{L_i}\right)^2\right], \quad i = 1, 2, 3 \tag{3}$$

Assuming the stiffening girder to be hinged at the supports, the boundary conditions at the support points are given by

$$v_i(0, t) = v_{g,i}(t), \quad v_i(L_i, t) = v_{i+1}(0, t) = v_{g,i+1}(t), \quad i = 1, 2, 3 \tag{4a}$$

$$v_i''(0, t) = 0, \quad v_i''(L_i, t) = v_{i+1}''(0, t) = 0, \quad i = 1, 2, 3 \tag{4b}$$

where, $v_{g,i}(t)$ and $v_{g,i+1}(t)$, respectively, represent the vertical ground displacements at the left and right supports of the ith span, and a prime ($'$) denotes the differentiation with respect to x_i.

To facilitate the solution of differential equations with these time-dependent boundary conditions, the quasi-static part may be separated from the dynamic component of the solution.[19] The total vertical deflection of a point on the ith span of the bridge may then be given by

$$v_i(x_i, t) = \sum_{j=1}^{4} g_{ji}(x_i) v_{g,j}(t) + \eta_i(x_i, t), \quad i = 1, 2, 3 \tag{5}$$

where, $g_{ji}(x_i)$ is the influence function for the displacement at x_i, due to unit vertical displacement at support, j, and $\eta_i(x_i, t)$ represents the dynamic component of the displacement response. The influence functions for a bridge can be determined uniquely by solving the boundary value problem obtained by substituting equation (5) in equation (1) and by separating the terms involving $g_{ji}(x_i)$ (see Reference 1 for details).

On considering the modal expansion of the dynamic component of response, we have

$$\eta_i(x_i, t) = \sum_{n=1}^{\infty} \phi_n(x_i)\xi_n(t), \quad i = 1, 2, 3 \tag{6}$$

where, $\phi_n(x_i)$ is the derived nth mode shape for the ith span of the bridge,[17,2] and $\xi_n(t)$ is the nth generalized co-ordinate. By virtue of the orthogonality of the mode shapes, the equation for the nth generalized co-ordinate may be written as

$$\begin{aligned}\ddot{\xi}_n + 2\zeta_n\omega_n\dot{\xi}_n + \omega_n^2\xi_n = &-2\zeta_n\omega_n\sum_{j=1}^{4} R_{jn}\dot{v}_{g,j}(t) - \sum_{j=1}^{4} R_{jn}\ddot{v}_{g,j}(t) \\ &+ P_n\alpha\sum_{k=1}^{3}\beta_k[v_{g,k}(t) + v_{g,k+1}(t)] \\ &- P_n\alpha[u_{g,4}(t) - u_{g,1}(t)], \quad n = 1, 2, 3, \ldots\end{aligned} \tag{7}$$

Copyright © 1999 John Wiley & Sons, Ltd.

where ζ_n and ω_n are the damping ratio and the natural frequency, respectively, in the nth mode, $\alpha = E_c A_c / L_e H_w$, $\beta_i = w_i L_i / 2H_w$, and $u_{g,1}(t)$ and $u_{g,4}(t)$ represent the longitudinal ground displacements at the first and the fourth support points, and R_{jn} and P_n are the participation factors given by

$$R_{jn} = \frac{\sum_{i=1}^{3} w_i \int_0^{L_i} g_{ji}(x_i)\phi_n(x_i)\,\mathrm{d}x_i}{\sum_{i=1}^{3} w_i \int_0^{L_i} \phi_n^2(x_i)\,\mathrm{d}x_i}, \quad j = 1, 2, 3, 4 \tag{8}$$

$$P_n = \frac{\sum_{i=1}^{3} w_i \int_0^{L_i} \phi_n(x_i)\,\mathrm{d}x_i}{\sum_{i=1}^{3} w_i \int_0^{L_i} \phi_n^2(x_i)\,\mathrm{d}x_i} \tag{9}$$

The first two terms on the right-hand side of equation (7) correspond to the modal forces that are proportional to the ground velocities and ground accelerations, respectively. The remaining two terms represent the modal forces which are proportional to the ground displacements, and are transferred to the stiffening girder through the cable-suspenders system. The presence of these latter terms differentiates the seismic analysis of a suspension bridge from that of a continuous girder highway bridge. Now, on transforming equation (7) to the frequency domain, we obtain

$$\Xi_n(\omega) = H_n(\omega)\Bigg\{ \sum_{j=1}^{4} (\omega^2 - 2\mathrm{i}\zeta_n\omega_n\omega) R_{jn} V_{g,j}(\omega) + P_n\alpha \sum_{k=1}^{3} \beta_k \{V_{g,k}(\omega) + V_{g,k+1}(\omega)\}$$

$$- P_n\alpha\{U_{g,4}(\omega) - U_{g,1}(\omega)\}\Bigg\}, \quad n = 1, 2, 3, \ldots \tag{10a}$$

where, $\Xi_n(\omega)$, $V_{g,j}(\omega)$, and $U_{g,j}(\omega)$ are the Fourier transforms of $\xi_n(t)$, $v_{g,j}(t)$, and $u_{g,j}(t)$, respectively, and $H_n(\omega) = 1/(\omega_n^2 - \omega^2 + 2\mathrm{i}\omega\omega_n\zeta_n)$ denotes the steady-state frequency response function for the nth mode of vibration. On rearranging the terms, equation (10a) becomes

$$\Xi_n(\omega) = H_n(\omega)\Bigg\{ \sum_{j=1}^{4} V_{g,j}(\omega)\{(\omega^2 - 2\mathrm{i}\zeta_n\omega_n\omega) R_{jn} + P_n\alpha\gamma_j\}$$

$$- P_n\alpha\{U_{g,4}(\omega) - U_{g,1}(\omega)\}\Bigg\}, \quad n = 1, 2, 3, \ldots \tag{10b}$$

with $\gamma_1 = \beta_1$, $\gamma_2 = \beta_1 + \beta_2$, $\gamma_3 = \beta_2 + \beta_3$, $\gamma_4 = \beta_3$. Equation (10b) can now be used to obtain the total displacement response of the ith span of the bridge in frequency domain as given by

$$V_i(x_i, \omega) = \sum_{j=1}^{4} g_{ji}(x_i)\, V_{g,j}(\omega) + \sum_{n=1}^{\infty} \phi_n(x_i)\Xi_n(\omega) \tag{11a}$$

which, on regrouping of various terms, may be written as

$$V_i(x_i, \omega) = \{\mathscr{H}_{V_i}(x_i, \omega)\}^{\mathrm{T}}\{\Delta_g(\omega)\} \tag{11b}$$

Here, $\{\mathscr{H}_{V_i}(x_i, \omega)\}$ represents the transfer function vector for the total displacement response of the suspension bridge, and $\{\Delta_g(\omega)\} = \{V_{g,1}(\omega), \ldots, V_{g,4}(\omega), U_{g,1}(\omega), U_{g,4}(\omega)\}^{\mathrm{T}}$ is the vector of free-field ground displacements. Similarly, the bending moment, $M_i(x_i, \omega)$, and the shear force,

Copyright © 1999 John Wiley & Sons, Ltd.

$Q_i(x_i, \omega)$, at any point in the ith span of the bridge may be obtained as

$$M_i(x_i, \omega) = \{\mathscr{H}_{M_i}(x_i, \omega)\}^{\mathrm{T}} \{\Delta_g(\omega)\} \tag{12a}$$

$$Q_i(x_i, \omega) = \{\mathscr{H}_{Q_i}(x_i, \omega)\}^{\mathrm{T}} \{\Delta_g(\omega)\} \tag{12b}$$

where $\{\mathscr{H}_{M_i}(x_i, \omega)\}(= E_i I_i(\mathrm{d}^2/\mathrm{d}x_i^2)\{\mathscr{H}_{V_i}(x_i, \omega)\})$ and $\{\mathscr{H}_{Q_i}(x_i, \omega)\}(= E_i I_i(\mathrm{d}^3/\mathrm{d}x_i^3)\{\mathscr{H}_{V_i}(x_i, \omega)\})$, respectively, are the transfer function vectors for the bending moment and shear force responses at a point in the ith span of the bridge.

The above formulation for the bridge response in frequency domain is based on the assumption that the bridge is rigidly anchored at its base. This will be extended in the next section to include the effects of dynamic SSI.

3. FORMULATION INCLUDING DYNAMIC SSI

The analysis including the dynamic SSI effects is complicated not only due to the frequency-dependent nature of the foundation impedances, but also because it is inconvenient to analyse the combined soil–structure system as a single system. Hence, it is considered convenient to use the sub-structure technique wherein the foundation and the super-structure are treated as two separate units with the interaction forces of equal magnitude acting in opposite directions on the two sub-systems. Since the dynamic SSI phenomenon is associated with a relative motion between the structural foundation and the compliant soil, it is possible to account for the dynamic SSI effects by analyzing a fixed-base structure which is subjected to a suitably modified ground motion.[13] The ground motion is modified to include the interaction accelerations developed at the soil–foundation interface. These accelerations are evaluated by relating the structural deformations to the relative displacements of the foundation by means of the impedance functions and by considering the dynamic equilibrium of the system. In this study, we extend this approach of Gupta and Trifunac[13] to the analysis of suspension bridges.

3.1. *Deterministic formulation*

On including the relative motions of the support foundations to the adjoining soil, the expressions for the total deformation, $V_i(x_i, \omega)$, the bending moment, $M_i(x_i, \omega)$, and the shear force, $Q_i(x_i, \omega)$, at a point on the stiffening girder in the ith span of the bridge, as in equations (11) and (12), may be written as

$$V_i(x_i, \omega) = \{\mathscr{H}_{V_i}(x_i, \omega)\}^{\mathrm{T}} \{\Delta_t(\omega)\} \tag{13a}$$

$$M_i(x_i, \omega) = \{\mathscr{H}_{M_i}(x_i, \omega)\}^{\mathrm{T}} \{\Delta_t(\omega)\} \tag{13b}$$

$$Q_i(x_i, \omega) = \{\mathscr{H}_{Q_i}(x_i, \omega)\}^{\mathrm{T}} \{\Delta_t(\omega)\} \tag{13c}$$

where, $\{\Delta_t(\omega)\} = \{V_{t,1}(\omega), \ldots, V_{t,4}(\omega), U_{t,1}(\omega), U_{t,4}(\omega)\}^{\mathrm{T}}$ is the vector of the vertical and longitudinal components of the total ground displacements (including the relative displacements of the foundations) at the supports. For example, $V_{t,j} = V_{g,j}(\omega) + V_{0,j}(\omega)$ and $U_{t,j} = U_{g,j}(\omega) + U_{0,j}(\omega)$

Copyright © 1999 John Wiley & Sons, Ltd.

are these displacement components at the jth support. Here, the subscript 'g' refers to the free-field translations modified for the kinematic interaction. If the effects of kinematic interaction are negligible, this refers to the free-field translations only. Further, the subscript '0' refers to the relative motions of the foundation due to SSI. Now, on considering the dynamic equilibrium of the jth support, we have

$$\omega^2 m_{bj} V_{t,j}(\omega) - Q_{j,L}(\omega) + Q_{j,R}(\omega) + R_{vj}(\omega) = 0 \tag{14a}$$

$$\omega^2 m_{bj} U_{t,j}(\omega) - H_{j,L}(\omega) + H_{j,R}(\omega) + R_{uj}(\omega) = 0 \tag{14b}$$

$$\omega^2 I_{bj} \Theta_{t,j}(\omega) + R_{\theta j}(\omega) = 0 \tag{14c}$$

where, m_{bj} and I_{bj} denote the mass and mass moment of inertia, respectively, of the foundation at the jth support; $\Theta_{t,j}(\omega)$ represents the rocking component of the total ground displacement at the jth support; $Q_{j,L}(\omega)$ and $Q_{j,R}(\omega)$ are the shear forces just to the left and right, respectively, of the jth support; and $H_{j,L}(\omega)$ and $H_{j,R}(\omega)$ denote the axial thrust in the girder (due to the horizontal component of the cable tension) just to the left and right, respectively, of the jth support. Further, $R_{vj}(t)$, $R_{uj}(t)$, and $R_{\theta j}$ are the interaction forces that are related to the relative displacements through the foundation impedance functions as

$$R_{vj}(\omega) = K_{vv}(\omega) V_{0,j}(\omega) \tag{15a}$$

$$R_{uj}(\omega) = K_{hh}(\omega) U_{0,j}(\omega) + K_{hr}(\omega) \Theta_{0,j}(\omega) \tag{15b}$$

$$R_{\theta j}(\omega) = K_{rh}(\omega) U_{0,j}(\omega) + K_{rr}(\omega) \Theta_{0,j}(\omega) \tag{15c}$$

where, $K_{vv}(\omega)$, $K_{hh}(\omega)$, and $K_{rr}(\omega)$ are the impedance functions for the vertical, longitudinal, and rocking motions, respectively, of the foundation, and $K_{hr}(\omega) = K_{rh}(\omega)$ is the impedance function for the coupling between the longitudinal and rocking motions. Further, $\Theta_{0,j}$ is the component of $\Theta_{t,j}(\omega)$ due to the dynamic SSI alone. It is equal to $\Theta_{t,j}(\omega)$ if the effects of kinematic interaction are negligible.

Now, on substituting equations (13) and (15) in equation (14) for each of the four supports and on simplifying, eight complex simultaneous equations are obtained which may then be solved for the interaction displacements at the support points at a given frequency of excitation. It may be noted that the equations corresponding to the longitudinal and rocking motions of the intermediate supports, as in equations (14b) and (14c), are omitted here as these motions do not lead to change in cable tension (cable runs continuously over the towers) and thus do not influence the structural response. In matrix form, these equations may be written as

$$[A(\omega)]\{\Delta_0(\omega)\} = [\mathscr{H}(\omega)]\{\Delta_f(\omega)\} + [F]\delta(\omega) \tag{16}$$

where, $[A(\omega)]$ is the 8×8 dynamic stiffness matrix, $\{\Delta_0(\omega)\} = \{V_{0,1}(\omega), \ldots, V_{0,4}(\omega), U_{0,1}(\omega), U_{0,4}(\omega), \Theta_{0,1}(\omega), \Theta_{0,4}(\omega)\}^{\mathrm{T}}$ is the vector of interaction displacements, $\{\Delta_f(\omega)\} = \{V_{g,1}(\omega), \ldots, V_{g,4}(\omega), U_{g,1}(\omega), U_{g,4}(\omega), \Theta_{g,1}(\omega), \Theta_{g,4}(\omega)\}^{\mathrm{T}}$ is the vector of modified free-field displacements (for kinematic interaction), and $[\mathscr{H}(\omega)]$ is the 8×8 transfer function matrix relating the modified free-field displacements to the interaction forces. Further, $\delta(.)$ represents the Dirac delta function, and $\{F\}$ is the 8×1 force vector due to dead loads only. $\{F\}$ comprises of the

Copyright © 1999 John Wiley & Sons, Ltd.

horizontal component of the cable tension, H_w, and the vertical reaction, P_w, at the tower tops due to the cable tension. If the effects of kinematic interaction are negligible, $\Theta_{g,j}(\omega) = 0$ for $j = 1, 2, 3, 4$, and $[\mathscr{H}(\omega)]$ becomes a 8×6 matrix. On solving equation (16) for $\{\Delta_0(\omega)\}$ and on adding this to the vector of free field displacements, $\{\Delta_f(\omega)\}$, the effective input ground displacements at the base of the jth support may be expressed as

$$\{\Delta_t(\omega)\} = [\chi(\omega)]\{\Delta_f(\omega)\} + \{\bar{\Delta}_0\}\delta(\omega) \tag{17}$$

Here, $[\chi(\omega)]$ is the transfer function matrix relating the total displacements to the modified free-field displacements, and $\{\bar{\Delta}_0\}$ represents the interaction displacements caused due to the (dead-load) cable tension. These effective input motions may now be used in place of the free-field motions to compute the seismic response in frequency domain by using the formulation for rigidly supported suspension bridges as given in the previous section. It may be noted that this formulation does not depend upon the support rocking motions, and therefore, it is not necessary to solve for $\Theta_{0,1}(\omega)$ and $\Theta_{0,4}(\omega)$ while solving equation (16).

3.2. Stochastic formulation

The above formulation can be used to estimate deterministic seismic response of a suspension bridge, if the earthquake excitation is characterized in form of free-field time-histories at each support point. However, if the excitation is characterized through spectral matrix of the ground motion process, it is necessary to obtain the Power Spectral Density Function (PSDF) of the desired response process from the input spectral matrix. For example, the PSDF of the response process, $v_i(x_i, t)$, may be obtained as

$$G_{V_i}(x_i, \omega) = \{\mathscr{H}_{V_i}(x_i, \omega)\}^T [\chi(\omega)][G_{\Delta_f}(\omega)][\chi^*(\omega)]^T \{\mathscr{H}^*_{V_i}(x_i, \omega)\} \tag{18}$$

by using equations (13a) and (17), and on ignoring $\{\bar{\Delta}_0\}$ (since this is deterministic, its effects may be studied separately and superimposed with those of $\{\Delta_f(\omega)\}$). In equation (18), $[G_{\Delta_f}(\omega)]$ represents the specified spectral matrix of the free-field ground displacements. An element of this spectral matrix, e.g., the cross-PSDF between the ground motion components, $U_j(\omega)$ and $U_k(\omega)$, may be specified as

$$G_{U_jU_k}(\omega) = \sqrt{G_{U_j}(\omega) G_{U_k}(\omega)}\, \gamma_{jk}(\omega) \tag{19}$$

where, $G_{U_j}(\omega)$ and $G_{U_k}(\omega)$, respectively, denote the PSDFs of the ground displacements, $U_j(\omega)$ and $U_k(\omega)$, and $\gamma_{jk}(\omega)$ represents the coherency function for the horizontal ground motions at the two stations, j and k. The cross-PSDF will become identically zero if the two motions are uncorrelated, e.g. as in the case of free-field horizontal and vertical motions. It may be noted that since the Fourier transforms of the ground displacements are proportional to those of the ground accelerations, the coherency of the displacements is likely to be very close to that of the accelerations. Hence, a coherency function for ground accelerations will be used here to represent the coherency of the horizontal ground displacements. For convenience, the coherency model of Hindy and Novak[16] will be used. This function may however not be adequate to describe the spatial variation of vertical motions. Hence, in the absence of studies on the coherency of the vertical motions, it will be assumed in this study that the coherency function proposed by Hindy and Novak[16] is applicable for the vertical motions also.

Copyright © 1999 John Wiley & Sons, Ltd.

In the case of kinematic interaction being considered, it may not be convenient to directly characterize the (modified) free-field motions in form of PSDFs and coherency function. One may however obtain the modified time-histories corresponding to various sets of spatially correlated free-field time histories[8] and then use those to estimate the elements of spectral matrix in an ensemble average sense.

The time-independent PSDF of a response process, e.g. $G_{V_i}(x_i, \omega)$ as considered above, is applicable only when the response process is a stationary process. This happens only when the excitation process is stationary and no significant non-stationarity is introduced in the response due to the sudden application of the (finite-duration) excitation. The input ground acceleration processes are however strongly non-stationary, and therefore, it is proposed to replace those by 'equivalent stationary' processes which have the same Fourier spectrum shapes as those of the actual processes and correspond to specified values of expected peak ground acceleration (PGA).[14] The 'equivalent stationary' processes are assumed to have the same durations as the strong motion durations of the actual processes. Further, since the suspension bridges are highly flexible systems, the initial transient phase of a response to a stationary excitation cannot be assumed to be small in comparison to the steady-state part. Hence, it is proposed to obtain the evolutionary PSDF, $G_{V_i}(x_i, \omega, t)$, instead of $G_{V_i}(x_i, \omega)$, from the spectral matrix of the 'equivalent stationary' free-field ground motions. Such a PSDF may be conveniently obtained from $G_{V_i}(x_i, \omega)$ by replacing the modal damping, ζ_n, in the nth fixed-base mode by the fictitious time-dependent damping ratio, $\zeta_n(t)$ ($= \zeta_n/[1 - e^{-2\zeta_n\omega_n t}]$).[20] The evolutionary PSDF may now be used in the order statistics formulation of Shrikhande and Gupta[14] to estimate the peak amplitudes of desired orders (i.e. largest, second largest, third largest, etc.) for a specified confidence level. This formulation is a simple extension of the stationary formulation of Gupta and Trifunac[21] and Gupta[22] to evolutionary response processes.

4. NUMERICAL STUDY

4.1. Illustration of the proposed approach

The proposed formulation is used to compute the (probabilistic) seismic response of the Golden Gate Bridge located at San Francisco, California. The structural parameters of the bridge as considered in this analysis are the same as considered by Abdel-Ghaffar and Rubin[2] and as given in Table I. This has led to the same fixed-base natural frequencies, mode shapes, and the quasi-static influence functions as given by Abdel-Ghaffar and Rubin.[2] It may be mentioned that in this case, the anti-symmetric modes contribute negligibly to the dynamic response of the bridge. First 25 (symmetric) modes have been considered in this study with the fixed-base natural frequencies as 0·620, 0·744, 0·965, 1·605, 2·127, 2·529, 3·170, 3·638, 4·153, 5·058, 5·952, 6·629, 7·410, 7·726, 8·476, 12·029, 13·002, 14·577, 15·605, 17·415, 18·261, 19·048, 21·749, 23·825, and 27·461 rad/s. A constant damping ratio of 2 per cent has been assumed for all 25 modes, and the assumed parameters for the soil-foundation system are given in Table II. Though the assumed zero depth of embedment is unrealistic for various practical situations, this may still give qualitatively meaningful results.

As mentioned earlier, this study considers the coherency function,

$$\gamma_{jk}(\omega) = \exp(-\alpha\omega r_{jk}) \exp(-i\omega r_{jk}/v_{app}) \tag{20}$$

Copyright © 1999 John Wiley & Sons, Ltd.

Table I. Structural parameters of the Golden Gate Bridge

w_1, w_3	337·1 kN/m
w_2	331·3 kN/m
E_1, E_2, E_3	$2{\cdot}0 \times 10^5$ MPa
I_1, I_3	3·35 m^4
I_2	5·2 m^4
L_1, L_3	343·0 m
L_2	1280·0 m
A_c	1·07 m^2
E_c	$2{\cdot}0 \times 10^5$ MPa
H_w	$4756{\cdot}7 \times 10^5$ kN
P_w	$2453{\cdot}5 \times 10^5$ kN
L_e	2300·0 m

Table II. Assumed soil–foundation parameters

Mass of foundation, m_b	$200{\cdot}0 \times 10^5$ kg
Radius of foundation, r_b	20·0 m
Embedment, e	0·0 m
Density of soil, ρ	1890·0 kg/m^3
Poisson's ratio, v	0·35

as given by Hindy and Novak.[16] In equation (20), α denotes the incoherence factor for the random field, r_{jk} represents the distance between the jth and kth supports, and v_{app} is the apparent velocity of propagation of the seismic wave-front. The parameters α and v_{app}, respectively, have been assumed to be 0·0001 and 2500 m/sec for the purpose of illustration. It may be mentioned that any other coherency model (e.g., that proposed by Harichandran and Vanmarcke,[23] Hao *et al.*[24] or Der Kiureghian[25]) could have as well been considered in place of equation (20). However, this model has been chosen because of its simplicity which makes the interpretation of results easier. Further, the Fourier spectra of the horizontal and vertical motions at each support point have been considered to be consistent with the pair of USNRC design spectra for 2 per cent damping and 0·1g (horizontal) PGA. It may be noted that these Fourier spectra correspond to those expected ground motions which are realistic with respect to non-stationarity in amplitude and frequency content, besides being consistent with the specified design spectra.[26] These Fourier spectra thus represent the energy distribution in the expected motions in 'temporal average' sense only as would happen in case of recorded accelerograms being available in place of design spectra. For this reason, two different cases of realistic accelerograms have been considered corresponding to (1) Case I — the S00E and vertical component records of the Imperial Valley Earthquake of May 14, 1940 as recorded at the El Centro site with the strong motion duration (i.e. 90 per cent duration as defined by Trifunac and Brady[27] of 24·42 sec, and (2) Case II — the synthetically generated horizontal and vertical components of the Michoacan Earthquake of 1985 for Mexico City site with the strong motion duration of 46·44 sec (see Reference 28 for details). It has been assumed that the horizontal and vertical free-field motions are uncorrelated. Also, the effects of kinematic interaction have been ignored, and the impedance functions given by Pais and

Copyright © 1999 John Wiley & Sons, Ltd.

Table III. Response estimates for the main span — Case I

Response	β (m/sec)	Time-hist.	Exp.	(5%)	(95%)
Max. disp. at mid-point (in m)	300	1·075	0·944	0·557	1·412
	900	1·131	1·004	0·599	1·488
Max. BM at mid-point (in 10^4 kN-m)	300	4·514	4·009	2·973	5·292
	900	4·467	4·003	3·025	5·229
Max. SF at quarter-point (in 10^2 kN)	300	6·223	5·661	4·419	7·205
	900	6·045	5·421	4·306	6·825

Table IV. Response estimates for the main span — Case II

Response	β (m/sec)	Time-hist.	Exp.	(5%)	(95%)
Max. disp. at mid-point (in m)	300	0·479	0·501	0·362	0·672
	900	0·612	0·581	0·417	0·785
Max. BM at mid-point (in 10^4 kN-m)	300	5·037	5·361	4·225	6·786
	900	4·876	5·179	4·077	6·571
Max. SF at quarter-point (in 10^2 kN)	300	6·137	6·996	5·721	8·612
	900	5·290	5·996	4·901	7·393

Kausel[15] have been used due to their simplicity and ease of application in modelling different types of foundation systems. Expected values of the maximum displacement and maximum bending moment at the mid-point of the centre span and the expected value of the maximum shear force at the quarter-point of the centre span as obtained by using the proposed approach have been shown in Tables III and IV, respectively, for the Case I (El Centro type) and Case II (Mexico City type) motions. Two values of shear wave velocity, 300 and 900 m/sec, have been considered corresponding to the medium soft and stiff soils for the purpose of illustration. Besides the expected values, the 5 and 95 per cent confidence level estimates of the response peaks have also been obtained to delineate the 90 per cent confidence interval.

Tables III and IV also show the ensemble-averaged time-history results, besides the probabilistic estimates. For the time-history results, two different ensembles of 20 spatially correlated, design spectrum-compatible ground acceleration time-histories have been synthesized by using the spectral decomposition technique and the phase characteristics of the accelerograms as in Cases I and II (see References 26 and 29 for details). For each set of sample time-histories at different supports, the responses have been computed in two steps by (i) calculating the interaction displacement time-histories at each support point by using equation (16), and (ii) by subjecting the (fixed-base) example bridge to the free-field and interaction displacement time-histories simultaneously.

Copyright © 1999 John Wiley & Sons, Ltd.

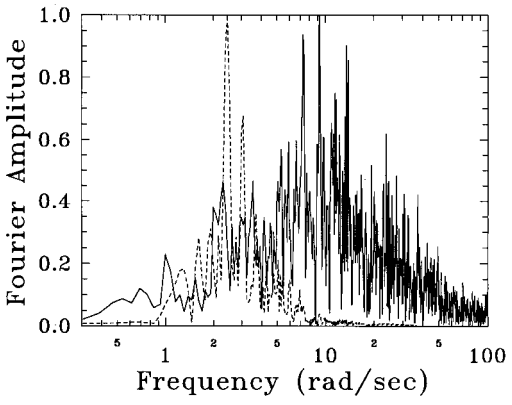

Figure 2. Normalized Fourier amplitude spectra of (i) Imperial Valley earthquake motion (solid line), and (ii) Michoacan earthquake motion (dashed line)

It may be seen from Tables III and IV that the expected peak values are in reasonably good agreement with those based on the time-history simulations. For most of the cases, the error is within 10%. This should be acceptable considering that the correlation structure of the generated accelerograms may not exactly match with that assumed for the probabilistic analysis.

4.2. Effects of dynamic SSI

To study the effects of dynamic SSI on the seismic response of the Golden Gate bridge, different soil conditions with β ranging from 50 (very soft) to 1000 m/sec (firm) have been assumed. For simplicity, no changes in impedance functions (except those due to changing β) have been considered, even though same type of foundation system may not be provided under the piers for this large variation in soil conditions. Two ground excitation processes have been considered corresponding to (i) the vertical and the S00E components of the Imperial Valley earthquake recorded at the El Centro site on 14 May, 1940, and (ii) the synthetically generated vertical and horizontal components of the Michoacan earthquake of 1985 at the Mexico City site (see Reference 28). In the case of Michoacan earthquake motions, most of the energy is concentrated within a narrow band of frequencies ($\sim$1–10 rad/sec), while the Imperial Valley earthquake motions are broad-banded with significant energy in the band of $\sim$0·25–100 rad/sec. The Fourier spectra for the horizontal components of these example excitations are compared in Figure 2. Following are the results of this numerical study.

4.2.1. SSI modification functions

We first consider the transfer functions, $\chi(\omega)$s, relating the modified ground displacements to the free-field ground displacements. Let the moduli of these transfer functions be called as SSI modification functions. The modification functions relating the modified vertical ground displacements to the imposed vertical displacements at the second support are shown in Figure 3(a) for various soil conditions. Similarly, Figure 3(b) shows the SSI modification functions relating the modified longitudinal ground displacements to the imposed longitudinal displacements at the first support. It may be noted that the nature of the SSI modification functions for the vertical

Copyright © 1999 John Wiley & Sons, Ltd.

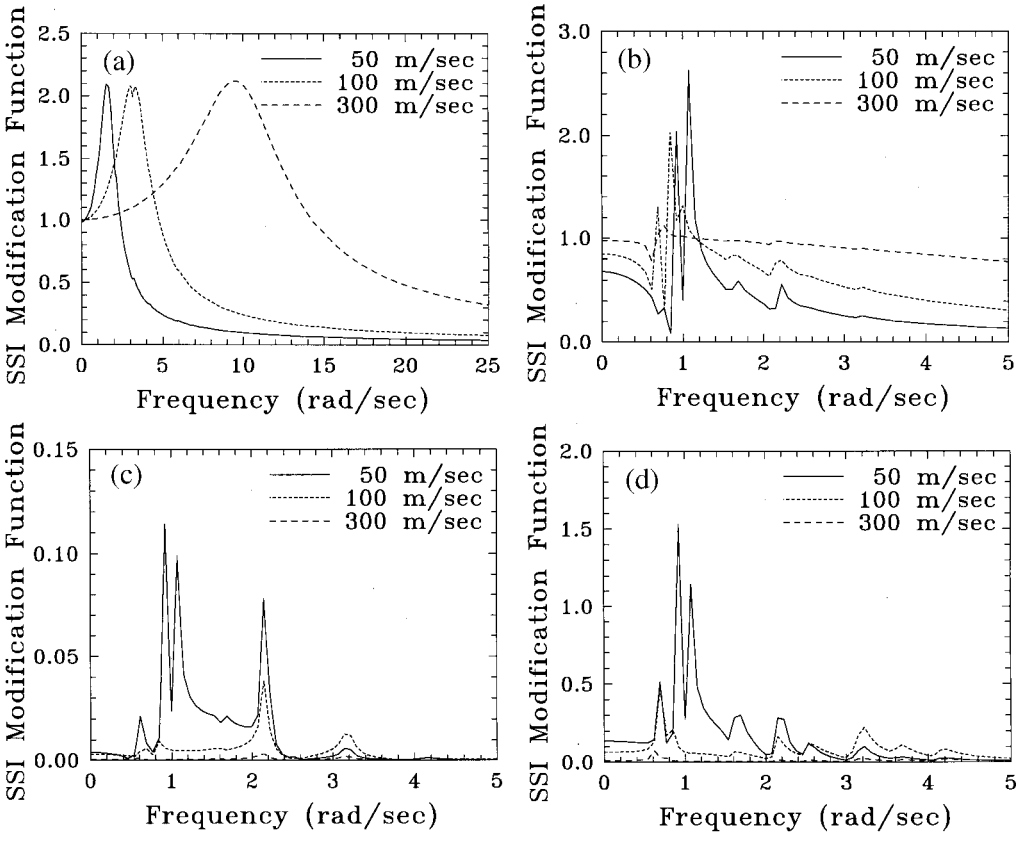

Figure 3. SSI modification functions for different β values for (a) vertical displacement due to imposed vertical displacement at the second support, (b) longitudinal displacement due to imposed longitudinal displacement at the first support, (c) vertical displacement at second support due to imposed longitudinal displacement at the first support, and (d) longitudinal displacement at first support due to imposed vertical displacement at the second support

motions is similar to that of the 'base acceleration to displacement response' transfer function of a SDOF oscillator (see Figure 3(a)). This suggests that the modifications of the imposed vertical ground displacements at a support, with other imposed displacements remaining zero, are caused mainly due to the compliance of the soil, and that the vibrations of the superstructure do not affect those significantly. On the other hand, the modification functions for the longitudinal ground displacements are significantly influenced by the structural vibrations as is evident from the presence of several peaks corresponding to the natural frequencies of the bridge. Actually, both longitudinal and vertical imposed displacements as considered in Figures 3(a) and 3(b) cause significant changes in the cable tension and thus cause vibrations in the bridge superstructure. These vibrations, in turn, change the cable tension. Since the longitudinal interaction displacements at the first support are much more sensitive to any changes in the cable tension, these effects of bridge vibrations (on cable tension) are reflected in Figure 3(b) instead of Figure 3(a). The observation that the vertical interaction displacements may be relatively insensitive to the changes in cable tension will be illustrated later.

Copyright © 1999 John Wiley & Sons, Ltd.

It may be further observed from Figure 3(b) that at zero frequency, the curves for lower shear wave velocities approach the smaller values of modification function following greater displacements of the anchor blocks relative to the surrounding soil. In fact, in the limit, the value of 1·0 corresponding to 'no modification' in the applied longitudinal displacement should be achieved for the rock-like soil conditions while the value of 0·5 (with equal displacement at the other anchor block) corresponding to 'no effect' of the applied longitudinal displacement on cable tension should be achieved for the extremely soft soil conditions. This reduction in the modified displacement for the softer soils is also observed at the other frequencies of excitation, except for the first few natural frequencies of the structural system. This may not however cause a corresponding reduction in the contribution of the longitudinal free-field displacements to the total structural response with increasing soil compliance because the earthquake ground displacements usually have energy in the frequency range, 0·5–2·0 rad/sec, and this range happens to contain the first few natural frequencies of the system. On comparison of Figure 3(b) with Figure 3(a), it may be noted that the peak occurring at the frequency of $\sim 1{\cdot}1$ rad/sec in the curve for $\beta = 50$ m/sec corresponds to the resonant frequency of the vertical soil spring at the second support. This suggests that there may be significant vertical motions at the second support when the first support is imparted longitudinal displacements. With the increase in β, this peak shifts to the higher frequencies and should be visible if the generated vertical motions are significant enough. This is shown more clearly in Figure 3(c) where, the SSI modification functions relating the interaction vertical displacements at the second support to the imposed longitudinal ground displacements at the first support are plotted for various soil conditions. It is also observed both from Figures 3(b) and 3(c) that with increasing SSI, the third and fifth modes of the structure start dominating the total response (see the large peaks at $\sim 0{\cdot}92$ and $\sim 2{\cdot}1$ rad/sec). The second mode has moderate contribution while the first and the fourth modes appear to have negligible contributions. This shows a remarkably different behaviour of the structure as compared to the fixed-base case when the first mode contributes significantly to the total response.

To see how sensitive are the vertical interaction displacements to the changes in cable tension, the SSI modification functions relating the longitudinal interaction displacements at the first support to the imposed vertical displacements at the second support are shown in Figure 3(d) for different soil conditions. It may be noted that even though these modification functions are similar to those in Figure 3(c) in terms of peaks at different frequencies, these functions have much greater amplitudes (about ten times) compared with those in Figure 3(c). Since the cable tension changes due to the imposed displacements in both cases, the vertical interaction displacements are evidently much less sensitive to these changes. It can be thus said that a greater transfer of energy should take place from the vertical free-field motions at the second support to the SSI-induced longitudinal motions at the first support than from the longitudinal free-field motions to the SSI-induced vertical motions.

4.2.2. Bending moment transfer functions

Next, we consider the steady-state transfer functions relating the bending moment (BM) response at the mid-point of the centre span of the bridge to the ground motion displacements at various supports. These transfer functions may be seen to be summations of the fixed-base response transfer functions, corresponding to different ground motion displacements, as scaled by appropriate χ's. The transfer function moduli corresponding to the longitudinal ground displacement at the first support (TF_1), and for the vertical ground displacement at the second support (TF_2) are compared in Figures 4(a) and 4(b), respectively, for the fixed-base case and for the bridge

Copyright © 1999 John Wiley & Sons, Ltd.

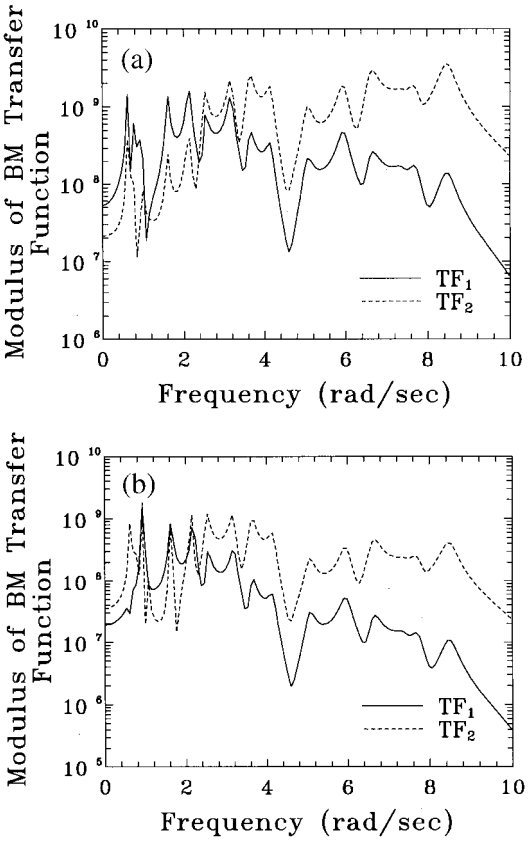

Figure 4. Comparison of BM transfer functions corresponding to TF_1 and TF_2 for (a) $\beta = \infty$ (fixed-base), and (b) $\beta = 50$ m/sec

founded on soft soil with $\beta = 50$ m/sec. It can be seen that in the case of the fixed-base structure, the amplitudes of the transfer function for the imposed longitudinal ground displacements are consistently higher than those for the imposed vertical ground displacements in the low frequency range (< 2 rad/sec). Considering that the free-field ground displacements are dominated by this range, longitudinal ground displacements should have greater contribution to the overall bending moment response. Similar observations have been made earlier by Abdel-Ghaffar and Rubin,[2] and Hyun *et al.*[6] This situation may however change in case of increased SSI. It is clear from Figure 4(b) that the transfer function amplitudes for the imposed vertical ground displacements are greater at the frequencies lower than 1 rad/sec. Actually, in case of significant SSI, imposed vertical displacements at the second support cause significant longitudinal interaction displacements at the first support, particularly in the frequency range of 0·5–2·5 rad/sec (see Figure 3(d)), and these displacements in turn cause additional bending moments. It may be further seen from Figures 4(a) and 4(b) that compared to the fixed-base case, the transfer functions in case of soft soil conditions are dominated by different ranges of exciting frequencies. This may be due to the increased importance of the third and fifth structure modes as observed above. The

Copyright © 1999 John Wiley & Sons, Ltd.

comparison of Figures 4(a) and 4(b) also shows that with the increasing soil interaction, frequencies greater than the first few dominant frequencies of the structure, say beyond 4 rad/sec in the present case, contribute lesser and lesser to the bending moment response. This is consistent with the fact that due to the modification by the soil interaction, the input ground displacements to the fixed-base structure are significantly reduced at these frequencies (see Figures 3(a) and 3(b)).

4.2.3. Effects of spatial variation of ground motion

The spatial variation of seismic ground motions has been modelled by equation (20) with the apparent velocity of propagation, v_{app}, and the incoherence factor, α, as the input parameters. Though v_{app} is a function of the velocity of the shear waves in the soil and the angle of incidence of the waves, it is common to calculate this and α from the recorded data of an array and to assume suitable values for the given site depending on how well it compares with the sites for which the array data are available. It is expected that with more array data becoming available in future, it will be possible to establish direct correlation of these parameters with the known source and site parameters. For a reasonable parametric variation here, four values of v_{app}, i.e. 1500, 2500, 3500 m/sec, ∞, and three values of α, i.e. 0, 0·0001, and 0·001, have been considered. It may be noted that the combination of $\alpha = 0{\cdot}0$ and $v_{app} = \infty$ corresponds to the case of uniform motion at each support. In this situation, the cable tension is not affected by the longitudinal free-field motions at the supports, and thus, the seismic response of the fixed-base bridge is fully governed only by the vertical ground motions at the supports. Further, the effects of wave propagation alone are considered when $\alpha = 0{\cdot}0$ and $v_{app} \neq \infty$, i.e. when the motions at a support point are merely time-delayed records of the motions at the adjacent supports.

The effects of wave propagation on the 'expected' BM response at the mid-point of the centre span of the bridge are shown for the El Centro and Mexico City motions in Figures 5(a) and 5(b), respectively, for varying shear wave velocity, β (and $\alpha = 0$). In each figure, the response estimates for each value of v_{app} are normalized with respect to that in case of the fixed-base structure to emphasize the SSI effects (which are more pronounced for greater deviations of the response amplification from unity). Due to this, all curves approach unity for the high values of β. It may be seen that the response amplification due to SSI is considerably influenced by the velocity of wave propagation, and for the range of parameters considered in the present study, maximum response amplification at a shear wave velocity is obtained in the case of uniform excitation. It may be noted that in this case, the (effective) input motions at various supports are not identical as would be the case with the fixed-base suspension bridge, and therefore, the longitudinal free-field motions also become important despite this being the case of uniform excitation. As the excitation becomes more and more non-uniform and the free-field displacements at different supports have greater phase differences, this response amplification generally appears to become lesser and lesser. Further, as seen from the comparison of the figures for the two example excitations, the trend of variation in the response amplification with β is affected by the energy distribution in the incident seismic waves. As seen in the preceding section, the frequency-dependent contributions of the imposed displacements at the support points to the response function depend significantly on the shear wave velocity, particularly for the soft soils. Within the frequency range of interest, the shifting of the peaks corresponding to the structural modes may not be significant. However, depending on how the free-field displacements are modified for the SSI (see Figures 3(a)–3(d)) in the dominant frequency range ($\sim 0{\cdot}5$–$1{\cdot}0$ rad/sec) of the excitation, some of the free-field displacements may become more important than the other displacements thus leading to an increased or decreased response. Following the discussion on the transfer functions for the BM response as

Copyright © 1999 John Wiley & Sons, Ltd.

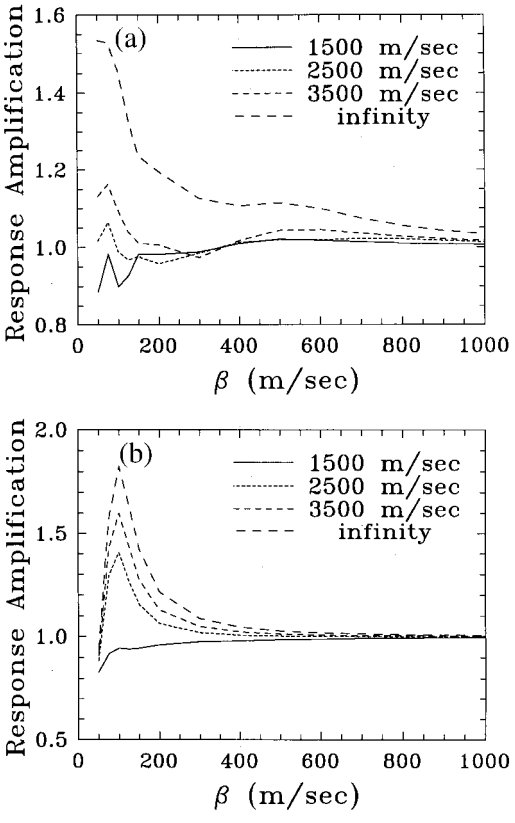

Figure 5. Comparison of BM response amplification (due to SSI) for different v_{app} values in case of (a) Imperial Valley earthquake motion, (b) Michoacan earthquake motion, and $\alpha = 0$

above, it may be generally true that as the soil becomes softer, the individual contributions of the vertical free-field displacements at the supports keep on increasing with no significant change in the contributions of the longitudinal displacements. Due to this, the response amplification due to SSI for a fixed value of v_{app} increases for lower values of β. However, below a certain value of $\beta = \beta_{crit}$, the contributions of the longitudinal displacements suddenly drop due to the higher modes (with frequencies > 1 rad/sec) dominating the response. This causes a sudden drop in the response amplification with the decreasing shear wave velocity for $\beta < \beta_{crit}$. For the cases considered here, β_{crit} is observed to be ~ 100 m/sec. It may be observed that this trend of variation in response amplification with β is more prominent in case of 'not so uniform' as compared to the case of uniform excitations. For the curves corresponding to $v_{app} = 1500$ m/sec, the effects of wave propagation considerably affect the contributions of the free-field displacements at different supports due to the changes in the relative phases between them. In fact, it may be seen in Figure 5(b) that the response amplification factor monotonically decreases for this apparent velocity with the decrease in the shear wave velocity.

The effect of the ground motion incoherence on the response amplification due to SSI for the two example excitations is shown in Figures 6(a) and 6(b), respectively. There are three curves in

Copyright © 1999 John Wiley & Sons, Ltd.

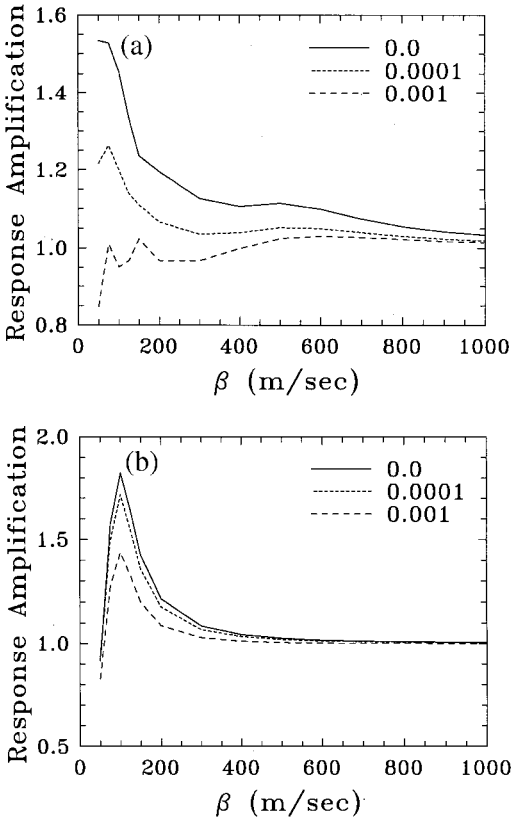

Figure 6. Comparison of BM response amplification (due to SSI) for different α values in case of (a) imperial valley earthquake motion, (b) Michoacan earthquake motion, and $v_{app} = \infty$

each figure corresponding to the three values of the incoherence factor, $\alpha = 0$, 0·0001, and 0·001, and a constant value of $v_{app} = \infty$. It can be seen that the effect of variation of ground motion incoherence is quite significant and similar in nature to that of v_{app}, for a given shear wave velocity. In this case, however, the phase differences between the free-field displacements at different supports are of random nature.

It follows from the above discussion that with an increase in the spatial variability of free-field ground motions either due to the wave propagation or incoherence, the bridge response becomes less sensitive to the dynamic interaction. This should be particularly true when the embedment effects of the foundations are also taken into account. However, it should be noted that different trends may be obtained when the ground motions have spatial variability due to both wave propagation and incoherence. In fact, depending upon how the relative phases caused by these two phenomena combine, we may have a value of α for which the variation in v_{app} has negligible effect on the response amplification for a shear wave velocity. Similarly, there may be a value of v_{app} for which the variation in α does not affect the response amplification factor. To illustrate, such two cases are considered for the Mexico city motions. Figure 7(a) shows the response amplification vs β curves for different v_{app} values and $\alpha = 0{\cdot}001$, while Figure 7(b) shows these

Copyright © 1999 John Wiley & Sons, Ltd.

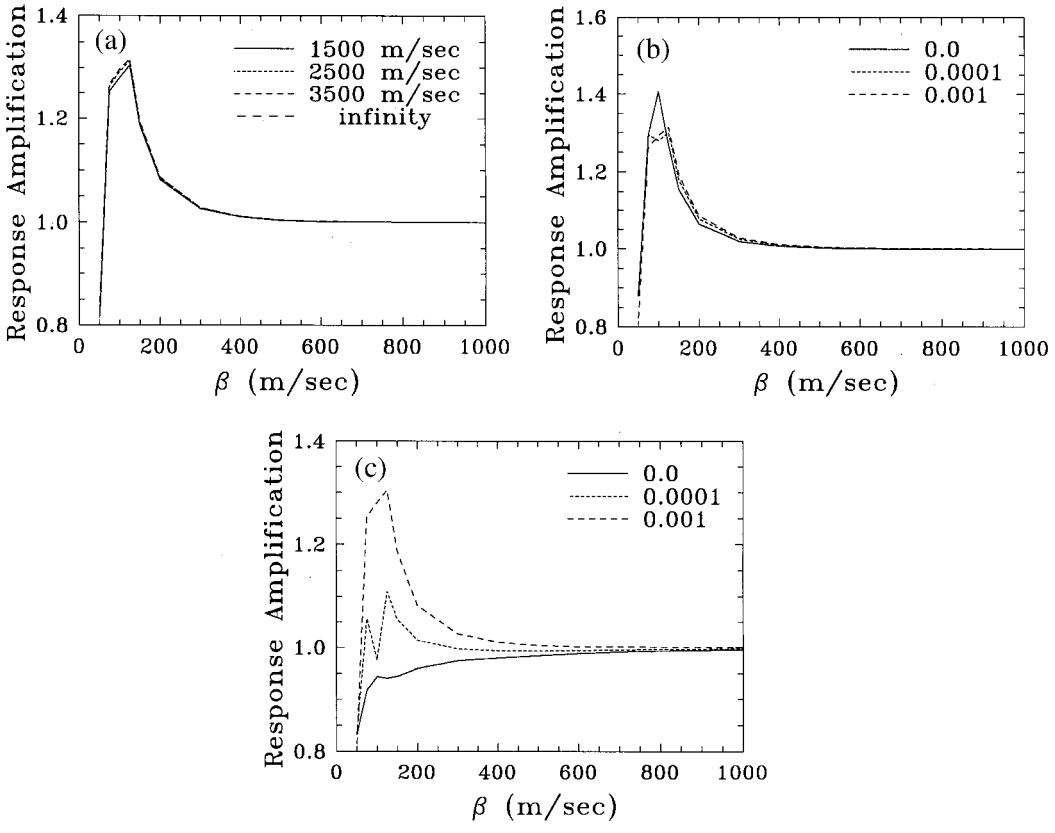

Figure 7. Comparison of BM response amplification (due to SSI) in case of Michoacan earthquake motion for (a) different v_{app} values and $\alpha = 0{\cdot}001$, (b) different α values and $v_{app} = 2500$ m/sec, and (c) different α values and $v_{app} = 1500$ m/sec

curves for different α values and $v_{app} = 2500$ m/sec. In the latter case, if v_{app} is instead chosen as 1500 m/sec, greater effect of SSI on response amplification is obtained for greater incoherence. As seen in Figure 7(c), this is in contradiction with the observations for Figure 6(b). In general, the ground motions have both propagation delay and incoherence, and thus, it is not obvious that how significant the response amplifications due to SSI are likely to be for a given combination of α and v_{app}. However, since there are several combinations of these parameters which may lead to substantial amplification or deamplification of response for soft soils (say, $\beta < 200$ m/sec), the effects of dynamic SSI should not be ignored in general.

5. CONCLUSIONS

A stochastic approach has been formulated for estimating the linear seismic response of a suspension bridge supported on a compliant soil. Though the proposed formulation is developed for a three-span bridge, it can be easily extended to apply in other cases as well. The

Copyright © 1999 John Wiley & Sons, Ltd.

key features of the proposed formulation are that (i) the modelling of the ground excitation process has been simplified by considering an 'equivalent stationary' process having a desired value of PGA, (ii) the formulation directly accounts for the non-stationarity in the transient phase of structural response, (iii) it is based on the use of the fixed-base modes of the bridge, and that (iv) it can be used to estimate the peaks of higher orders with a given level of confidence. The excitation process is characterized by the Fourier amplitude spectra and a suitable coherency function for the expected vertical and horizontal ground motions at the site. The proposed formulation has been illustrated by analyzing the example suspension bridge for two different earthquake excitations. In both cases, the 'expected' largest peak responses as estimated by using the proposed formulation have been found to be in good agreement with the 'ensemble-averaged' results of the time-history analyses.

A comprehensive SSI analysis would also include the kinematic interaction effects which are caused by the scattering of the traveling seismic waves at the soil–structure interface. Since the kinematic interaction essentially modifies the (free-field) foundation input motion, the proposed formulation can still be used provided the Fourier amplitude spectra and the phase differences between the modified input motions at different support foundations are known. Moreover, the proposed formulation can also be used for the analysis of any multiple-support structural system with/without embedded foundations by merely changing the foundation impedance functions and the transfer function vectors for the system response. Although the proposed formulation considers the vibrations of a suspension bridge in the vertical plane only, this can be easily extended to accommodate a three-dimensional model of the structural system.

The proposed formulation has been used to study the dynamic SSI effects on the seismic response of Golden Gate bridge. It has been found on considering two different ground motion processes that the contributions of the vertical ground displacements to the bridge response increase with increasing soil compliance, while those of the longitudinal ground displacements may be reduced for very soft soil conditions due to the reduced participation of the lower modes in the total response. This observation may not change significantly even when more realistic impedance functions are considered since the impedance functions for the vertical degree of freedom are relatively insensitive to the depth of embedment. This study also shows that the response amplification due to the dynamic SSI effects may depend significantly on the degree of spatial variation in the seismic ground motions at a site. More and more uniform and coherent the motions at different supports are, more will be the response amplification due to dynamic SSI. These conclusions on SSI effects are however based on a simple model of the suspension bridge with identical soil conditions at all the supports. A more realistic model including the longitudinal and lateral bridge vibrations and softer soil conditions at the intermediate supports should be considered for quantitatively more meaningful results.

REFERENCES

1. A. M. Abdel-Ghaffar and L. I. Rubin, 'Suspension bridge response to multiple-support excitations', *J. Engng. Mech. Div.* ASCE **108**, 419–435 (1982).
2. A. M. Abdel-Ghaffar and L. I. Rubin, 'Vertical seismic behavior of suspension bridges', *Earthquake Engng. Struct. Dyn.* **11**, 1–19 (1983).
3. A. M. Abdel-Ghaffar and R. G. Stringfellow, 'Response of suspension bridges to travelling earthquake excitations: part I. Vertical response', *Soil Dyn. Earthquake Engng.* **3**, 62–72 (1984).
4. A. M. Abdel-Ghaffar and R. G. Stringfellow, 'Response of suspension bridges to travelling earthquake excitations: part II. Lateral response', *Soil Dyn. Earthquake Engng.* **3**, 73–81 (1984).
5. A. A. Dumanoglu and R. T. Severn, 'Stochastic response of suspension bridges to earthquake forces', *Earthquake Engng. Struct. Dyn.* **19**, 133–152 (1990).

Copyright © 1999 John Wiley & Sons, Ltd.

6. C.-H. Hyun, C.-B. Yun and D.-G. Lee, 'Non-stationary response analysis of suspension bridges for multiple support excitations', *J. Prob. Engng. Mech.* **7**, 27–35 (1992).
7. R. S. Harichandran, A. Hawwari and B. N. Sweidan, 'Response of long-span bridges to spatially varying ground motion', *J. Struct. Engng. ASCE* **122**, 476–484 (1996).
8. R. Betti, A. M. Abdel-Ghaffar and A. S. Niazy, 'Kinematic soil-structure interaction for long-span cable-supported bridges', *Earthquake Engng. Struct. Dyn.* **22**, 415–430 (1993).
9. Y. Yamada, H. Takemiya and K. Kawano, 'Random response analysis of non-linear soil-suspension bridge pier', *Earthquake Engng. Struct. Dyn.* **7**, 31–47 (1979).
10. H. Tajimi, 'Discussion: building-foundation interaction effects', *J. Engng. Mech. Div. ASCE* **93**, 294–298 (1967).
11. A. K. Chopra and J. A. Gutierrez, 'Earthquake response analysis of multistorey buildings including foundation interaction', *Earthquake Engng. Struct. Dyn.* **3**, 66–77 (1974).
12. I. D. Gupta and M. D. Trifunac, 'Probabilistic spectrum superposition for response analysis including the effects of soil–structure interaction', *J. Prob. Engng. Mech.* **5**, 9–18 (1990).
13. V. K. Gupta and M. D. Trifunac, 'Seismic response analysis of multistoried buildings including the effects of soil–structure interaction', *Soil Dyn. Earthquake Engng.* **10**, 414–422 (1991).
14. M. Shrikhande and V. K. Gupta, 'A generalized approach for the seismic response of structural systems', *Eur. Earthquake Engng.* **XI**(2), 3–12 (1997).
15. A. Pais and E. Kausel, 'Approximate formulas for dynamic stiffnesses of rigid foundations', *Soil Dyn. Earthquake Engng.* **7**, 213–227 (1988).
16. A. Hindy and M. Novak, 'Response of pipelines to random ground motions', *J. Engng. Mech. Div. ASCE* **106**, 339–360 (1980).
17. A. M. Abdel-Ghaffar, 'Suspension bridge vibration: continuum formulation', *Proceedings of the 1980 ASCE* convention, Portland, Oregon, April 14–18, 1980. Reprinted in *J. Engng. Mech. Div. ASCE* **108**, 1215–1232 (1980).
18. A. M. Abdel-Ghaffar, 'Vertical vibration analysis of suspension bridges', *J. Struct. Engng. Div. ASCE* **106**, 2053–2075 (1980).
19. R. D. Mindlin and L. E. Goodman, 'Beam vibrations with time-dependent boundary conditions', *J. App. Mech. ASME* **17**, 377–380 (1950).
20. E. H. Vanmarcke, 'Structural response to earthquakes', in C. Lomnitz and E. Rosenblueth (eds), *Seismic Risk and Engineering Decisions*, Elsevier, Amsterdam, 1976, pp. 287–337.
21. I. D. Gupta and M. D. Trifunac, 'Order statistics of peaks in earthquake response', *J. Engng. Mech. Div. ASCE* **114**, 1605–1627 (1988).
22. V. K. Gupta, 'Higher order peaks in seismic response of multistoried buildings', *Report No. 94-03*, Dept. of Civil Engg., I.I.T. Kanpur, India, 1994.
23. R. S. Harichandran and E. H. Vanmarcke, 'Stochastic variation of earthquake ground motion in space and time', *J. Engng. Mech. Div. ASCE* **112**, 154–174 (1986).
24. H. Hao, C. S. Oliviera and J. Penzien, 'Multiple-station ground motion processing and simulation based on SMART-1 array data', *Nucl. Engng. Des.* **111**, 293–310 (1989).
25. A. Der Kiureghian, 'A coherency model for spatially varying ground motions', *Earthquake Engng. Struct. Dyn.* **25**, 99–111 (1996).
26. M. Shrikhande and V. K. Gupta, 'Generating ensembles of design spectrum-compatible accelerograms', *Eur. Earthquake Engng.* **X**(3), 49–56 (1996).
27. M. D. Trifunac and A. G. Brady, 'A study on the duration of strong earthquake ground motion', *Bull. Seismol. Soc. Am.* **65**, 581–626 (1975).
28. V. K. Gupta and M. D. Trifunac, 'Response of multistoried buildings to ground translation and rocking during earthquakes', *J. Prob. Engng. Mech.* **5**, 138–145 (1990).
29. M. Shrikhande and V. K. Gupta, 'On synthesizing ensembles of spatially correlated accelerograms', *J. Engng. Mech. ASCE* **124**(11), 1185–1192 (1998).

Copyright © 1999 John Wiley & Sons, Ltd.